

Supplementary Materials for

**Intermittent Low-Magnitude Pressure Applied Across Macroencapsulation Devices Enables Physiological Insulin Delivery Dynamics**

Ella A. Thomson, Sooyeon Lee, Haixia Xu, Hannah Moeller, Joanna Sands, Rayhan A. Lal, Justin P. Annes, Ada S. Y. Poon

Corresponding to: [adapoon@stanford.edu](mailto:adapoon@stanford.edu) and [jannes@stanford.edu](mailto:jannes@stanford.edu)

**This PDF file includes:**

Supplementary Methods

Supplementary Figs. 1 to 9

Supplementary Tables 1 to 2

**Other Supplementary Materials for this manuscript includes the following:**

Supplementary Movie 1

Supplementary CAD files 1 to 2

## Supplementary Materials

### Time required to transport 90% of secreted insulin out of a cell chamber

Solving Fick's diffusion equation, the time constant for one-dimensional diffusion across a membrane is

$$\tau = \frac{Vh}{AD_s} \quad (1)$$

where  $V$  is the volume of the cell chamber,  $A$  is the open membrane area,  $h$  is the membrane thickness, and  $D_s$  is the insulin diffusion coefficient. The time constant is proportional to the thickness of the cell chamber ( $V/A$ ). Transporting 90% of secreted insulin out of the cell chamber takes approximately 2.3 time constants.

### Derivation of multiplicative effect of applied pressure relative to diffusion for insulin transport

We start by considering the combined effect of a concentration and a pressure gradient on solute transport across a porous membrane. The combined insulin flux is dependent on flux due to solute diffusional flow, and volumetric solvent flow. This is given by

$$J_s = J_v c_s - D_s \nabla c_s. \quad (2)$$

The solute diffusional flow  $-D_s \nabla c_s$  is driven by the insulin concentration gradient,  $D_s$  is the solute specific diffusion coefficient, and  $\nabla c_s$  is the concentration gradient. The insulin flux,  $J_v c_s$ , due to solvent flow is pressure-dependent, with  $J_v$  given by

$$J_v = -L_p h \nabla p. \quad (3)$$

Here,  $L_p$  is the filtration coefficient and  $h$  is the membrane thickness. We can substitute Eq. 3 into Eq. 2 and yield

$$J_s = -L_p h \nabla p \cdot c_s - D_s \nabla c_s. \quad (4)$$

Considering a one-dimensional problem for equation Eq. 4, normalized to membrane thickness, we obtain

$$J_s = -L_p \frac{dp}{dx} c_s - \frac{D_s}{h} \frac{dc_s}{dx}. \quad (5)$$

Under steady state conditions, the fluxes due to both pressure and concentration gradients are independent of  $x$ . This gives a homogeneous second order differential equation:

$$\frac{d^2 c_s}{dx^2} - P_e \frac{dc_s}{dx} = 0 \quad (6)$$

Solving the differential equation in Eq. 6 gives

$$c_s = ae^{Pe^x} + b. \quad (7)$$

Applying the boundary conditions ( $c_{s,in} = a + b$  and  $c_{s,out} = ae^{-Pe} + b$ ), we can solve for  $a$  and  $b$ :

$$a = -\frac{(c_{s,in} - c_{s,out})e^{-Pe}}{1 - e^{-Pe}} \quad (8)$$

$$b = \frac{c_{s,in} - c_{s,out}e^{-Pe}}{1 - e^{-Pe}}. \quad (9)$$

Substituting our solution for  $c_s$  to Eq. 5, with  $Pe = \frac{L_p h \Delta p}{D_s}$  gives

$$J_s = J_v \frac{c_{s,in} - c_{s,out}e^{-Pe}}{1 - e^{-Pe}}. \quad (10)$$

We then take the ratio of combined pressure and diffusion transport to diffusion only transport to yield Eq. 4 in the main text.

### Expressing axial Peclet number in terms of applied pressure and membrane properties

The axial Peclet number is given by

$$Pe = \frac{L_p h \Delta p}{D_s}. \quad (11)$$

We can apply the Hagen-Poiseuille Law to obtain

$$L_p = \frac{\varepsilon r_p^2}{\tau 8 \eta h} \quad (12)$$

where  $\varepsilon$  is the porosity,  $\tau$  is the tortuosity, and  $r_p$  is the pore radius of the membrane,  $h$  is the membrane thickness, and  $\eta$  is the viscosity of water. For insulin transport where membrane pore radius ( $r_p$ ) is much greater than molecular radius of insulin ( $r_s$ ), we can apply the Stokes-Einstein equation to obtain

$$D_s \approx \frac{\varepsilon k_B T}{\tau 6 \pi \eta r_s} \quad (13)$$

where  $k_B$  is the Boltzmann constant and  $T$  is the absolute temperature. Substituting Eq. 12, 13 into Eq. 11, and simplifying yield Eq. 6 in the main text.

### Design of the PET membrane cell encapsulation implant for *in vivo* experiments and cell culture insert for *in vitro* experiments

Cell encapsulation implants were designed in FreeCAD and 3D printed using Fictiv PLA. Each implant consists of an 11-mm hollow cylinder with a closed end (Supplementary Fig. 6a) and features a 2-mm diameter tapered circular opening on the side for tubing (Supplementary Fig. 6b). The open end includes a 9-mm diameter circular opening for membrane attachment (Supplementary Fig. 6c). For pressure-driven insulin release experiments, a piezoelectric pump and controller were connected via the tubing. PET membranes (Sterlitech PET0413100) were affixed using polyester adhesive (Hotmelt Infinity IM-Supertac-500-12). The silicone tubing (McMaster-Carr Catalog #51845K52) has an inner diameter of 0.040 inches and an outer diameter of 0.085 inches. To sterilize the assembled inserts, we submerged them in 70% ethanol overnight.

For the cell culture insert, it was designed to fit into the well of a 12-well plate, and was also designed in FreeCAD and 3D printed using Fictiv PLA. It features a 9-mm diameter circular opening for membrane attachment and a 2-mm diameter tapered circular opening on the opposite side for tubing (Supplementary Fig. 1b). Wells were filled with 3 mL of media or water for experiments.

CAD files for both devices are provided in the Other Supplementary Materials.

### **Culturing and characterizing R7T1 $\beta$ -cells**

Immortalized mouse R7T1  $\beta$ -cells were cultured in high glucose DMEM with 4 mM L-glutamine, 1 mM sodium pyruvate, 10% FBS, 1% penicillin/streptomycin, and 1 mg/mL doxycycline. R7T1 cells (passage 10–34) were growth-arrested for 5 days in doxycycline-free medium with tetracycline-free FBS. Cells were authenticated by immunofluorescence staining with antibodies for insulin (1:500; Cell signaling), Pdx-1 (1:200; Cell signaling), and ZnT8 (1:50; Santa Cruz Biotechnology). For pseudoislet formation, growth-arrested R7T1 cells were plated at 300,000 cells per well in a 12-well non-adherent plate; pseudoislets were picked and counted after 16–24 hours.

R7T1 cells were characterized by comparing insulin secretion from growth-arrested and proliferating cells. Growth-arrested cells were cultured without doxycycline for 5 days, while proliferating cells were maintained with doxycycline. Both cell types were plated at 300,000 cells per well in a 12-well plate and cultured in low glucose DMEM (with or without doxycycline) for 24 hours. Media was replaced with high glucose media, and supernatant samples were collected after 30 minutes. Insulin content was measured by ELISA.

### **Human islet information and culture**

Human islets were obtained from the Alberta Diabetes Institute Islet Core (Pro00013094) or the Integrated Islet Distribution Program and used with approval from Stanford University's Administrative Panel on Biosafety. Islets were cultured overnight in islet medium before experiments. Donor information is in Supplementary Tables 1 and 2.

### **Islet viability experiments**

Human islets (200  $\mu$ L, 667 IEQ/cm<sup>2</sup>) were encapsulated and cultured in 12-well plates for 5 days. The pressure treatment group received 11 kPa for 30 seconds every 24 hours. Viability was assessed by collecting, trypsinizing, and staining the islets with trypan blue (Corning) at various time points. Cell viability was measured on days 1, 3, and 5, and normalized to day 0.

### **Mouse islet isolation**

Primary mouse islets were isolated from WT C57BL/6J mice (6–12 weeks old) by pancreatic perfusion. Pancreata were perfused with Cizyme RI (VitaCyte), digested at 37°C for 13 minutes, and islets were purified in a 5:6 Histopaque®-1077 and 1119 mixture. Islets were collected from the interface, filtered through a 70- $\mu$ m strainer, and cultured overnight in islet medium (low glucose DMEM with L-glutamine, sodium pyruvate, 10% FBS, and penicillin/streptomycin) before experimental use.

### **Histological analysis**

Mouse skin tissue surrounding the implant was harvested, fixed in 4% paraformaldehyde overnight, and embedded in paraffin. Deparaffinized and rehydrated sections (5  $\mu$ m) were stained with H&E or Masson's trichrome. For immunofluorescence, sections were antigen retrieved with citrate buffer (pH 6.0) in a pressure cooker for 10 min, blocked with 0.5% donkey serum/0.3% Triton X-100/PBS at room temp for 1 hour, and incubated overnight at 4°C with primary antibodies, F4/80 (1:500; Proteintech), CD31 (1:500; Proteintech), CD45 (1:500; Proteintech). Secondary antibodies (Jackson ImmunoResearch) were used for visualization and sections were imaged on a Leica DMIL inverted fluorescence microscope.

### **STZ diabetes induction and monitoring**

Eight-week-old male C57BL/6J mice were fasted for 4–6 hours. Streptozotocin (STZ) [100 mM] was prepared in sterile sodium citrate buffer (pH 4.5) and injected intraperitoneally: 175 mg/kg for non-survival and 150 mg/kg for survival experiments<sup>1,2</sup>. Mice received 10% sucrose in drinking water for three days post-injection to prevent hypoglycemia. Mice with non-fasting blood glucose >350 mg/dL were used for insulin dosing experiments within one week of STZ injection. Mice with blood glucose >450 mg/dL received 0.05–0.1 units of insulin subcutaneously daily, with the last dose at least 14 hours before experiments.

### **Design of piezoelectric pump controller and wearable wireless micropump**

Piezoelectric micropumps (Servoflo mp6-liq/mp6-hyb) were used for pressure-driven experiments. A pump driver and controller were designed, incorporating an electroluminescent lamp circuit (Microchip HV861) as a dual-output piezoelectric driver. Pump rate was calibrated by characterizing the frequency, duty cycle, and flow rate relationship.

For the wearable wireless micropump, a wireless module (Fanstel BC832) controlled the piezoelectric driver. The pump rate was adjusted via duty cycle, and pump time was set using a smartphone interface. The system was powered by a single lithium-ion (CR1616) battery. Silicone tubing (McMaster 2124T2) connected the pump to a polyolefin (Pointool PO-01450) reservoir. The pump fluid was either saline or cell culture media. The power consumption and weight were optimized for comfort in both wild type and STZ-induced diabetic mice. The miniaturized system was packaged in a wearable cotton pouch (Fig. 5e).

Pump pressure was characterized using a differential pressure sensor (NXP MPX2102DP) with a full-scale pressure of 100 kPa. The pump outlet was connected to the pressure sensor inlet using silicone tubing (McMaster 2124T3). Pressure was calculated based on sensor specifications and measured output voltage. For system pressure measurements, a 3D-printed encapsulation implant with a porous PET membrane and two openings for silicone tubing was used. The pump was connected to one tube, and the pressure sensor was connected to the other.

## References

1. Deeds, M. C. *et al.* Single dose streptozotocin-induced diabetes: considerations for study design in islet transplantation models. *Lab Anim* **45**, 131–140 (2011).
2. Furman, B. L. Streptozotocin-Induced Diabetic Models in Mice and Rats. *Curr Protoc Pharmacol* **70**, 5.47.1-5.47.20 (2015).

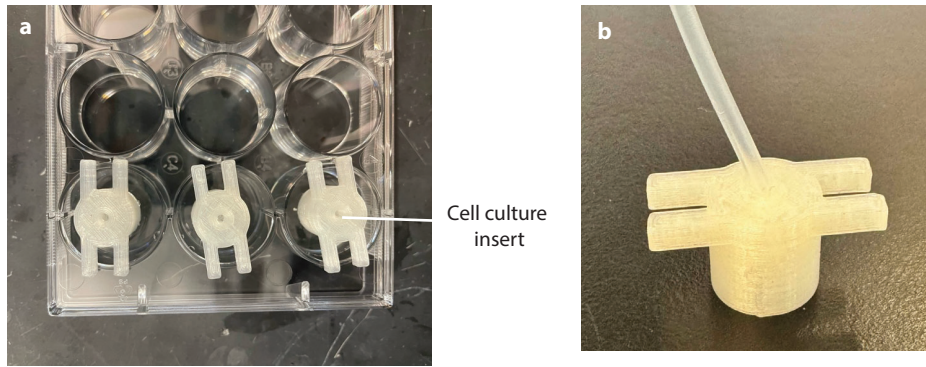


**Fig. 1. *In vitro* cell culture setup for insulin transport measurement.** (a) Photograph displays the custom cell culture inserts utilized for experimentation in a 12-well plate format, facilitating the measurement of insulin transport across a porous membrane. (b) Photograph displays the custom cell culture inserts with the silicon tubing inserted.

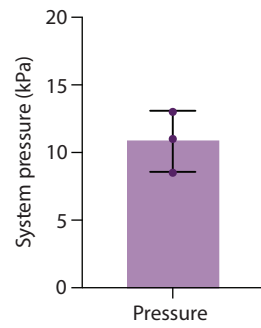


**Fig. 2. Measured pressure at porous membrane driven by the custom-designed piezoelectric micropump system.** Measured pump pressure across three different assembled pump systems.



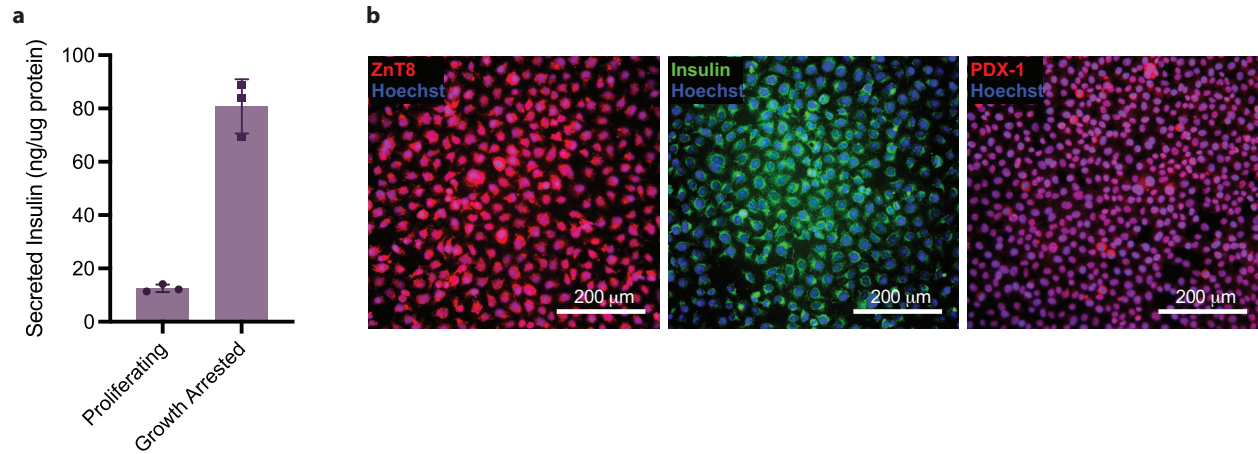


**Fig. 3. Characterization of R7T1  $\beta$ -cells.** **a**, Glucose stimulated insulin secretion from growth arrested and proliferating R7T1 cells. Secreted insulin was measured in response to 30 minutes of glucose [25 mM] stimulation after a period of 5 days of growth arrest or non-growth arrested controls,  $n = 3$ . **b**, Immunohistochemical staining of R7T1  $\beta$ -cells for identity markers including ZnT8, Insulin, and PDX1.

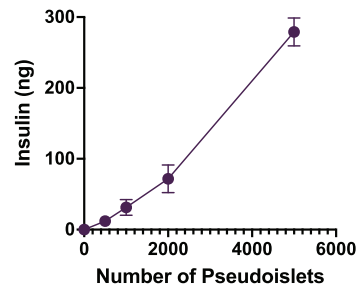


**Fig. 4. Effect of islet number on insulin release.** Insulin released into supernatant by pseudoislet numbers from 0 to 5000 was quantified by rodent insulin ELISA.

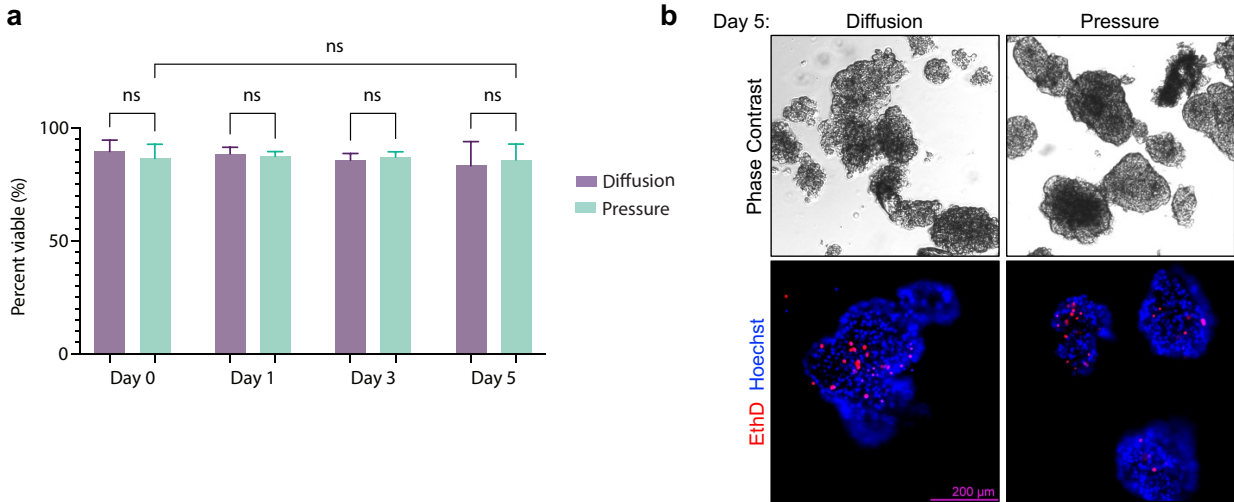


**Fig. 5. Human islet viability in encapsulation with and without daily applied pressure. a,** Measured viability for a period of 5 days and performed a pressure-driven dose once per day. **b,** Representative images of intact islets collected from encapsulation after 5 days of diffusion or applied pressure. Top, brightfield imaging. Bottom, immunofluorescence staining of cell death marker, Ethidium Homodimer (EthD; red) and Hoechst (blue).

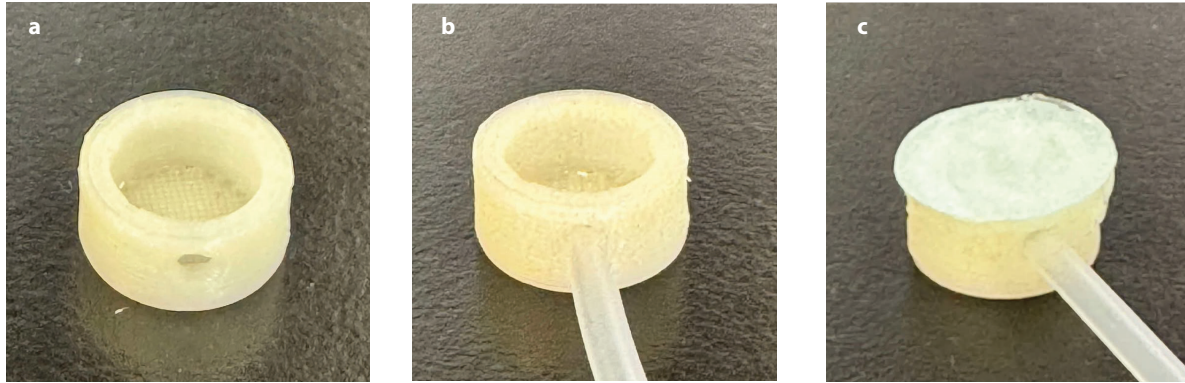


**Fig. 6. Cell encapsulation implant.** Photographs illustrating the assembly process of the cell encapsulation implant: **a**, a 3D-printed hollow cylinder with a closed end, designed to hold cells, featuring a 2-mm diameter tapered circular opening on the side. **b**, Silicon tubing inserted into the 2-mm diameter tapered circular opening. **c**, A membrane affixed to the open end of the cylinder.

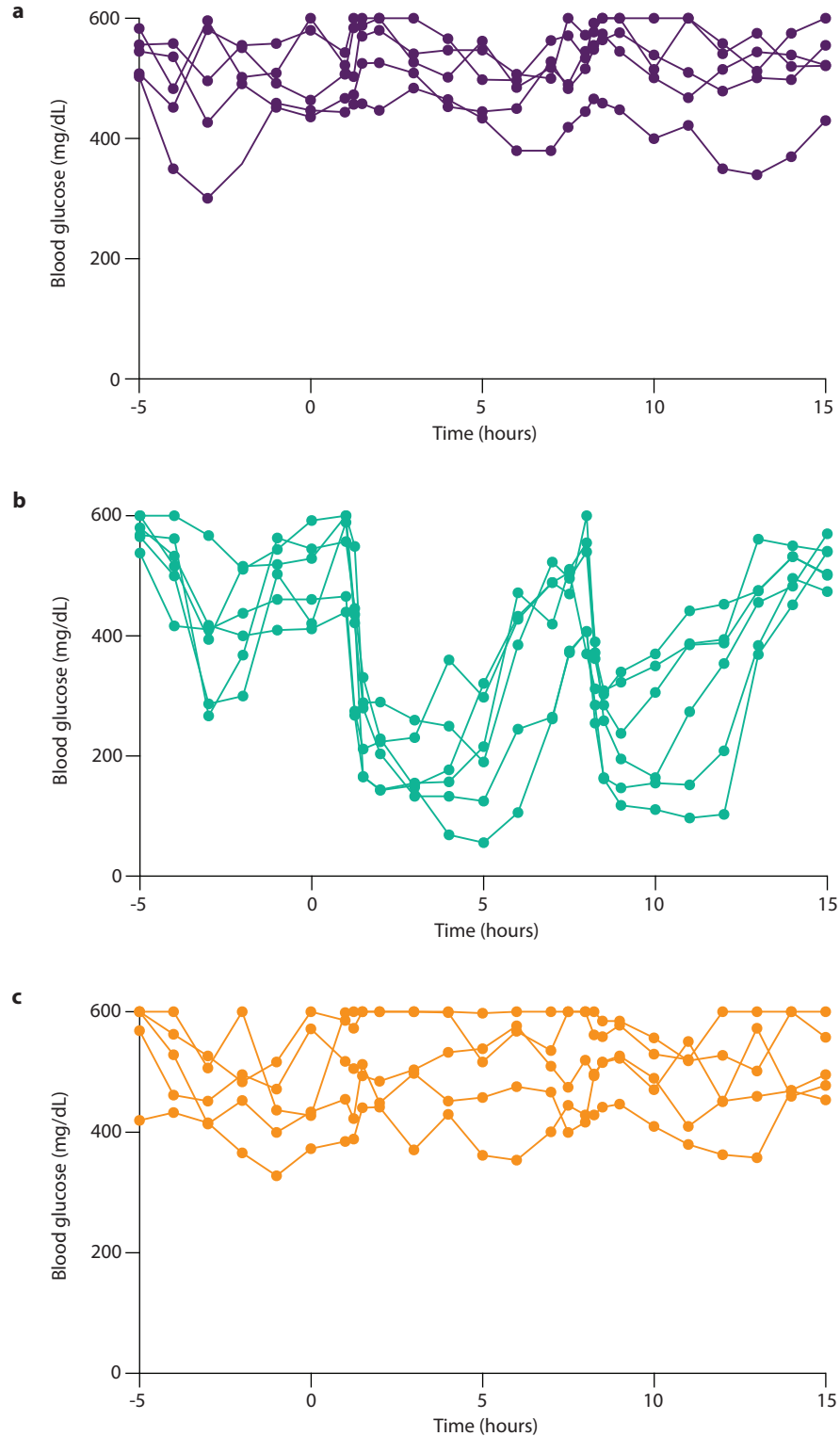


**Fig. 7. Raw blood glucose values from 2-dose insulin boluses experiment in Fig. 5b–d of the main text. a**, Raw blood glucose values for mice treated with insulin dosed via diffusion,  $n = 5$ . **b**, Raw blood glucose values for mice treated with insulin dosed via applied pressure,  $n = 6$ . **c**, Raw blood glucose values for sham mice,  $n = 5$ .

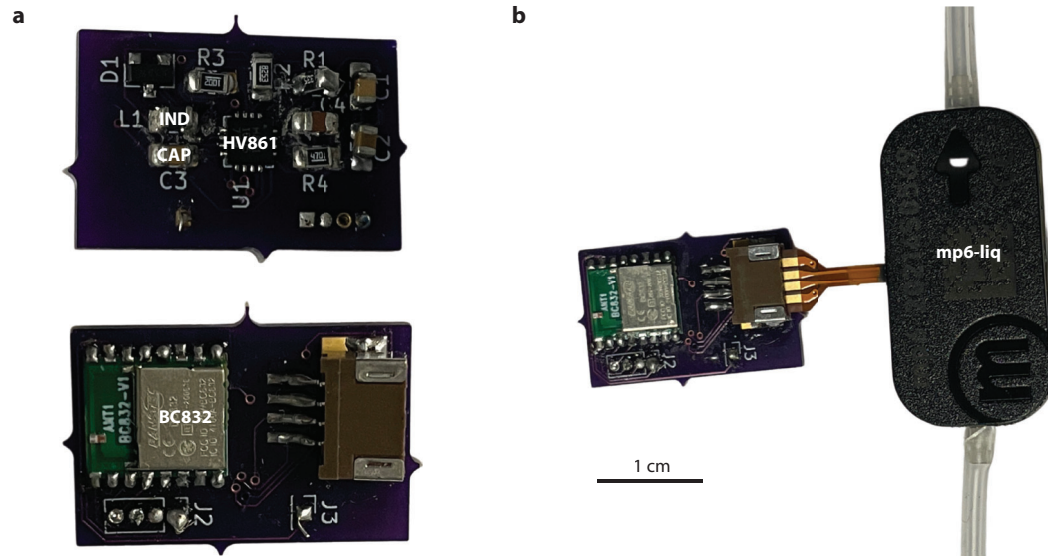


**Fig. 8. Wireless micropump system.** **a**, Photographs of the front (top) and reverse (bottom) sides of the pump control printed circuit board. The front side includes a high-voltage dual driver (part no. HV861), an inductor (IND), and a few other circuit components for the operation of the driver. The reverse side includes a Bluetooth transceiver module (part no. BC832) and a connector to the piezoelectric micropump. **b**, Photographs of the whole wireless micropump system including the piezoelectric micropump (part no. mp6-liq).

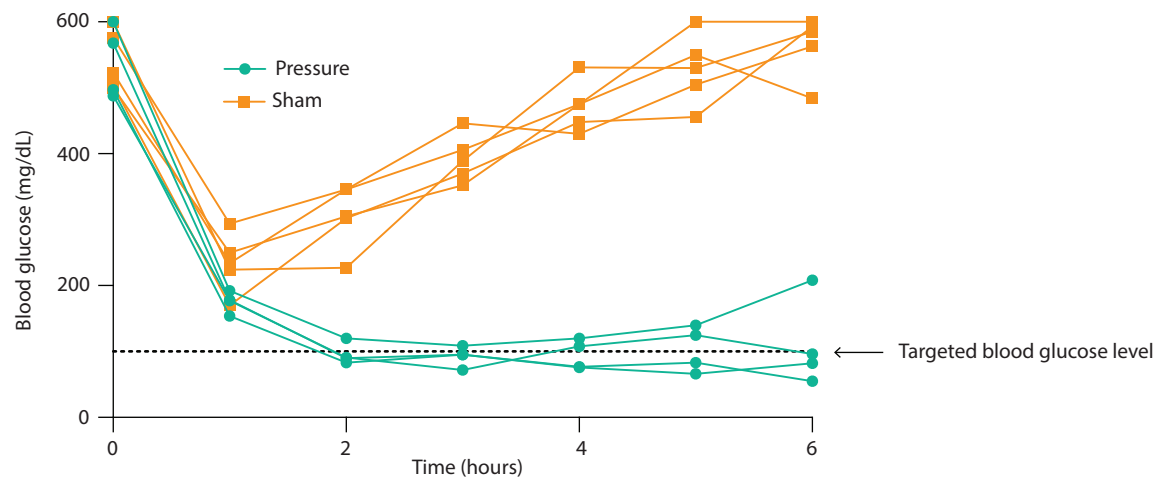


**Fig. 9. Raw blood glucose values from basal dosing experiment in Fig. 6h of main text.** Raw blood glucose values for mice treated with basal insulin dosing. Pressure,  $n = 4$ ; Sham,  $n = 5$ .

**Table 1: Donor information for the human islets obtained from the Alberta Diabetes Institute (ADI) IsletCore.** HbA1c, glycated hemoglobin; BMI, body mass index; RRID, research resource identified.

<b>Donor</b>	<b>1</b>	<b>2</b>	<b>3</b>
<b>Gender</b>	Female	Female	Male
<b>HbA1C (%)</b>	5.4	5.4	5.8
<b>Age (years)</b>	33	60	55
<b>BMI (kg/m<sup>2</sup>)</b>	31.9	25.9	23.5
<b>RRID</b>	R426	R421	R420
<b>Cold Ischemia Time (h)</b>	4	18.5	3.5



**Table 2: Donor information for the human islets obtained from the Integrated Islet Distribution Program (IIDP).** HbA1c, glycated hemoglobin; BMI, body mass index; RRID, research resource identified.

<b>Donor</b>	<b>1</b>	<b>2</b>	<b>3</b>	<b>4</b>	<b>5</b>
<b>Gender</b>	Male	Male	Male	Male	Male
<b>HbA1C (%)</b>			4.9		5.4
<b>Age (years)</b>	38	52	32	39	16
<b>BMI (kg/m<sup>2</sup>)</b>	28.4	37.5	26.9	32.4	29.5
<b>RRID</b>	SAMN30 181459	SAMN31 242270	SAMN31 815644	SAMN30 686018	SAMN32 641505
<b>Cold Ischemia Time (h)</b>	5.12	18.5	11.57	7.17	6.12